HEAT TRANSFER PERFORMANCE OF MHD NANOFLUID FLOW IN CORRUGATED ENCLOSURES WITH DIFFERENT INTERNAL HEAT SOURCE CONFIGURATIONS

Nowras Saad Abd Own[1]
eng747.naweras.saad@student.uobabylon.edu.iq
[1]Mechanical Engineering, University of Babylon

Isam Mejbel Abed[2]
eng.isam.m@uobabylon.edu.iq
[2]Mechanical Engineering, University of Babylon

ABSTRACT

The natural convection in a corrugated enclosure with the porous medium and filled with nanofluid with magnetic field was investigated. The numerical method was used to obtain the stream function for several inclinations of the magnetic field (γ = 0°, 45°, and 90°). The Darcy number that was a function of the range from 10^{-3} to 10^{-5}, was maintained and Rayleigh (Ra = 10^6) and Hartmann, Ha =60) numbers held fixed. The intensities of the fluid circulation strength were found to increase with increasing (γ), and maximum stream function strength was obtained at γ = 90°. Further, increasing the permeable resistance (decreasing Da) decreased fluid flow and suppressed natural convection. The overlay of the contours of temperature and streamline points to the contributions of both magnetic alignment and porous resistance in heat transfer. These findings emphasize the necessity of selecting appropriate magnetic orientation and porosity value to enhance maximum thermal efficiency in magneto-convective engineering systems.

Keywords: Magneto-natural convection-enclosure-nanofluid-Hartmann number-Nusselt number.

NOMENCLATURE

A	Amplitude	Ha	Hartmann Number
$C_{1\varepsilon}$, $C_{2\varepsilon}$	Model Constant	Pr	Prandtls Number
Cp	Specific Heat (kJ/kg. K)	Ra	Rayleigh Number
E	Trapezoidal Heater Position	Nu	Local Nusselt Number
g	Gravitational Acceleration (m/s^2)	α	Thermal diffusivity (m^2/s)
k	Thermal Conductivity (W/m. K)	β	Volumetric Coefficient of Thermal Expansion (K^{-1})
N	Number of Corrugations	γ	Magnetohydrodynamic Angle
P	Dimensionless Pressure	ε	Porosity
p	Pressure (Pa)	θ	Dimensionless Temperature (T-Tc/ΔT)
T	Temperature (K)	σ	Electrical Conductivity
U	Dimensionless Velocity Component X-Axis	Ψ	Dimensionless Stream Function

Received: August 8, 2025.
Accepted: December 28, 2025.

V	Dimensionless Velocity Component Y-Axis	ϕ	Nanofluid Volume Fraction
X	Dimensionless coordinate (horizontal direction)	μ	Dynamic viscosity (kg.s/m)
S	Minimum value equal to zero and maximum equal to 1	λ	Amplitude
F.E.M.	Finite Element Method	α	Thermal diffusivity, $m^{/s}$
TGC	Thermos Gravitational Convection	ε	Turbulent dissipation rate
MHD	Magnetohydrodynamics	υ	Kinematic viscosity of the fluid, m^2/s
Da	Darcy Number	ρ	Density, kg/m^3
Gr	Grashof Number	ϕ	Nanoparticle Volume Concentration
ξ	Volumetric Heat generation parameter	kna	Thermal Conductivity of Nanoparticle
kbf	Thermal Conductivity of Base Fluid	keff	Effective Thermal Conductivity of Nanofluid
Ω	Inclination Angle of the Magnetic Field		

INTRODUCTION

Due to the excellent empirical performance of nanofluids on convection, they have provided good research base for thermal systems in future Xuan and Li (2000). An analysis the heated square cavities filled with nanofluid was numerically carried out by Oztop and Abu-Nada (2008), they found that the location and dimension of the heated portion have a great effect on flow patterns as well as on heat transfer rate. Furthermore, the investigation of (Ghasemi and Aminossadati 2009) analysing the natural convection in a sinusoidal wavy enclosure with nanofluids demonstrated respectively that wall undulation promoted heat transfer attributes and nanoparticle concentration provided significant contributions as well. It was found significant combined effects for some combinations of amplitude and frequency. Muthtamilselvan, et al. (2010) studied the effect of wavy wall geometry with nanoparticles in convective heat transfer inside cavity. It is found that the wavy boundaries promoted the fluid mixing and its circulation, leading to increased overall thermal performance; moreover, this effect was potentiated by adding the nanoparticles at high Rayleigh numbers as well.

The effect of the variable, temperature-dependent thermophysical properties on natural convection in CuO–EG and water-based nanofluid has been investigated by Abu-Nada and Chamkha (2010), it is found that the viscosity plays a more important role on heat transfer characteristics than does thermal conductivity. Mahmoodi (2011) investigated the effects of Rayleigh number for wall corrugation on the natural convection in sinusoidal enclosure. The effect of nanoparticle concentration is to worsen, in general, thermal transfer and that end call corrugation amplitudes may be higher or lower thermal resistance according to what

the regime of Rayleigh number. Khanafer and Vafai (2011) emphasized on the effect of nanofluids, density and specific heat capacity, etc. with respect to particle type and size or concentration in terms of their significance in the applied aspect for the understanding of convective heat transfer augmentation. Ching-Chang, et al. (2013), studied the natural convection of water-based nanofluids in a wavy enclosure and found that particles can enhance heat transfer, with the changed shape of the enclosure and temperature distribution.

Moreover, Grobler et al., (2015) showed that simultaneous application of porous media and nanofluid is capable to increase the heat transfer efficiency remarkably taking place when these mechanisms are simultaneously presented in the same system. An investigation was performed of natural convection through a triangular cavity containing Cu–Al2O3 nanofluid subject to the positioning of a heat source and internal heating, Hartmann numbers, Rayleigh numbers and magnetic field effect (Rashad et al., 2018). They concluded that the Lorentz forces induced considerable changes in flow pattern and thermal transport with less heat transfer enhancement as compared to ordinary nanofluids. The flow of magnetohydrodynamic nanofluid passing through a permeable media was investigated and it was observed that porous material embedded with nanofluids results in 18% enhancement in the heat transfer by Sheikholeslami and Ganji (2017). A numerical study of natural convection heat transfer in U-shaped cavities with nanofluids. The average Nusselt number over surfaces showed the role of the Rayleigh number and the shape of enclosure. Detailed flow and temperature distribution patterns for various Rayleigh numbers were studied using $Al_2\ O_3$ –water nanofluid. The simulations were conducted using the commercial CFD software FLUENT, which utilizes finite volume calculations (Lotfi et al., 2018). Study of the natural convection of in a curved wavy cavity with nanofluid, has been scrutinized by FEM. The goal was to determine the impacts of wall undulation and cavity curvature on transport processes, with an opportunity for geometry design improvements in heat transfer performance. Mackolil and Mahanthesh (2021) studied an elliptic wavy enclosure filled with a heated circular cylinder, to obtain the influences of Darcy number, Rayleigh number, Hartmann number, nanoparticle volume fraction, magnetic field lean angle simultaneously on temperature profile and flow recirculation. Another work had found the optimal thermal Marangoni convection of a hybrid nanofluid by means of Response Surface Methodology (RSM). Thermal conductivity and viscosity results of the composite obtained from experiments were integrated into numeric model. It was shown in the analysis that these parameters as nanoparticles concentration, thermal radiation and exponent heat source intensity can enhance heat transfer rates. Improved thermal behavior was achieved with the nanoparticle fraction of less than 2%, where the factors radiation and the source had generated higher temperature gradients. It was observed that the highest radiation effects in addition to weaker exponential source of heat and smaller inclination angle in the magnetic field enhanced ($Nu \approx 7.46$). In addition, heat transfer inside wavy cavities filled with nanofluids was studied by a control-volume finite element approach which also indicated the important influence of wall geometry and heat transfer process.

This research showed that wavy wall feature caused admirable flow mixing and uniform thermal spreading consequently heat transfer increased Zahra, et al. (2020). The present study is conducted in both forced and mixed convection cases over a corrugated circular cylinder at two-dimensional steady laminar flow. The results showed that both corrugation number and amplitude exerted a significant influence on flow streamlines, isothermal contours and local as well as the average Nusselt numbers over the cylinder. More precisely,

at G = 5 and λ = 0.6, the heat transfer dropped by approximately 46% compared with smooth circular cylinder, as reported by Isam, et al. (2020). Heat transfer flow and pressure in wavy surface heat exchangers with nanofluid have been widely investigated. It has been reported that wavy surface configurations can enhance heat transfer rates by approximately 15–30% compared with flat-wall geometries, owing to improved mixing and thermal boundary-layer disruption. The study also revealed the synergistic effect of combining wavy geometric features along with nanofluids and recommended this approach in view of improving the performance of thermal systems. The Darcy and Rayleigh numbers are two indispensable dimensionless parameters that govern the heat convection in fluid filled cavities. The Rayleigh number, which quantifies the strength of natural convection, is defined as a ratio of buoyancy forces and viscous forces. The Darcy number is a key parameter characterizing the apparent permeability of the porous media, and it has been demonstrated to be crucial for imposition rules for flow problem in arbitrary geometries. The objective of this study is to observe the influence of Rayleigh and Darcy numbers on heat transfer characteristics in general within the enclosure. It also identifies the impacts of varying concentrations (1–5%) in fluid containing nanoparticles on thermal conductivity and heat transfer characteristics by comparing the trends obtained from wavy corrugated cavities with those derived from corn mandrel flat enclosures. These results are expected to be helpful for deploying more efficient thermal systems and energy resources (Zhang et al., 2022). A detailed numerical study has been conducted for free convection of nanofluid considering internal heating in a corrugated square cavity with a heat generating solid block. Darcy–Brinkman–Forchheimer model was used to simulate the porous medium flow and corrugated geometry influence is studied to understand its prospects in augmenting heat transfer. The results showed that the addition of nanoparticles and modification of the internal wall shape significantly enhances average Nusselt number. Furthermore, it was also observed that the amplitude and frequency of corrugation had significant impact on the strength of convective flow as well as on the entropy generation. This study contributes to the greater understanding for maximizing heat transfer systems via nanofluid flow and geometric alteration by Khan and Bilal (2025). Furthermore, Nehad et al. (2024) gave numerical and experimental studies for a diverging–converging enclosure possessing sinusoidal sidewalls which separated into two different regions under magnetohydrodynamic natural convection. The system included a core-centered and left-based corrugated cylinder made up of $Al_2 O_3 – C_2 H_6 O_2$ nanofluid and the right side was formed nanofluid and porous layer. Their findings have implications for engineering applications and investigated the influence of nanoparticle volume fraction, Darcy number, Rayleigh number, Hartmann number, magnetic field inclination angle on flow field pattern, temperature distribution and average Nusselt number in the presence of line heat sources as well as volumetric heat sources under three different configurations.

MATHEMATICAL MODELING

The mathematical modelling of the problem of natural convection filled with a nanofluid were included. The continuity, momentum and energy equations are solved assuming steady incompressible flow with negligible viscous dissipation. The effect of various internal heat-source geometries on the flow and heat transfer characteristics are investigated by employing the stream function and Nusselt number. Validation is performed by comparing with the available experimental data to check accuracy. The geometry of the

enclosure is shown in figure 1. In all such configurations, the sidewards regions of the cavity are occupied by and filled with Al_2O_3–water nanofluid; while the mid- region is manipulated as porous medium which accommodates heat generator. The configurations differ in the shape and location, as shown in figure 2.

- First: A circular heat source positioned at the midpoint of the porous layer.
- Second: A flower-shaped internal heat source placed within the same porous region.
- Third: A heated vertical boundary placed along the right wall of the enclosure, while the porous region remains in the center.

A more detailed comparison will be performed as the three configurations, to decide which configuration leads to the most robust fluid motion. The analysis is performed with the same physical parameters and boundary conditions so as to achieve an equitable comparison. The mathematical model based on the governing equations of natural convection with nanofluid. The continuity, momentum and energy equations are assumed to be solved under steady-state incompressible flow conditions with viscous dissipation taken as negligible. The effect of various internal heat-source configurations on the fluid flow and heat transfer is realizable through stream function and Nusselt number. The correctness of the validation is verified with some experimental data. The 2D model of the enclosure is shown in figure 1. In all cases, the side two zones of cavity are saturated with an Al_2O_3 - water nanofluid and the remaining central zone is filled by a porous media where heat source is placed. The differences between the configurations come from changes in shape of the heat source and location, as shown in figure 2.

PHYSICAL MODEL DESCRIPTION

The physical behavior inside the enclosure is represented using a set of assumptions that ensure numerical stability and an accurate description of the convection process. The enclosure consists of sinusoidally wavy vertical boundaries and a porous central region in which an internal heat source is embedded. The working fluid is $Al_2\ O_3$ –water nanofluid, while momentum transport within the porous medium is modeled using the Brinkman–Forchheimer extended Darcy formulation to capture both viscous and inertial resistance effects.

- The flow is steady, laminar, and incompressible, which is consistent with the moderate Rayleigh number range considered in this study.

- Heat transfer occurs purely by natural convection, and the thermophysical properties of the nanofluid are treated as constant throughout the domain.

- Density variation with temperature is incorporated only in the buoyancy term using the Boussinesq approximation, which provides a reliable description of natural convection effects without introducing unnecessary complexity.

Governing Equations

The natural convection process in the presence of a porous region in a nanofluid enclosure as below:

❖ **Continuity Equation:**

The mass preservation equation implies incompressibility

$$\frac{\partial u}{\partial x}+\frac{\partial v}{\partial y}=0 \quad (1)$$

❖ **Momentum Equations:**

The following momentum equation of natural convection which including Bowssinesq assumption is considered:

$$X-Momentum\ Equation$$

$$\rho_{nf}\left(u\frac{\partial u}{\partial x}+v\frac{\partial v}{\partial y}\right)=-C_1\frac{\partial p}{\partial x}+C_2\mu_{nf}\left(\frac{\partial^2 u}{\partial x^2}+\frac{\partial^2 u}{\partial y^2}\right)-C_3\mu_{nf}\frac{u}{K}+ C_1{B_o}^2\sigma_{nf}\left(Vsin(\gamma)cos(\gamma)-Usin^2(\gamma)\right) \quad (2)$$

$$Y-momentum\ Equation$$

$$\rho_{nf}\left(u\frac{\partial v}{\partial x}+v\frac{\partial v}{\partial y}\right)=-C_1\frac{\partial p}{\partial y}+C_2\mu_{nf}\left(\frac{\partial^2 v}{\partial x^2}+\frac{\partial^2 v}{\partial y^2}\right)-C_3\mu_{nf}\frac{v}{K}+C_1\rho_{nf}\beta_{nf}\,g\,(T-T_c)+ C_1{B_o}^2\sigma_{nf}\left(Usin(\gamma)cos(\gamma)-Vcos^2(\gamma)\right) \quad (3)$$

❖ **Energy Equation**

The following energy equation with behavior of the nanofluid is described as below:

$$u\frac{\partial T}{\partial x}+v\frac{\partial T}{\partial y}=C_4\left(\frac{\partial^2 T}{\partial x^2}+\frac{\partial^2 T}{\partial y^2}\right) \quad (4)$$

To formulate the non-dimensional governing relations, the corresponding dimensionless parameters as follows:

$$X=\frac{x}{H};\ Y=\frac{y}{H};\ A=\frac{L}{H};\ U=\frac{uH}{\alpha_{bf}};\ V=\frac{vH}{\alpha_{bf}};\ \theta=\frac{T-T_c}{(T_h-T_c)};\ P=\frac{pH^2}{\rho_{na}\alpha_{bf}^2};\ Pr=\frac{\nu_{bf}}{\alpha_{bf}};\quad Ra=\frac{g\beta_{bf}(T_h-T_c)H^3}{\alpha_{bf}\nu_{bf}};Da=\frac{K}{H^2};\ k_r=\frac{k_w}{k_{na}};Ha=B_oH\sqrt{\frac{\sigma_{na}}{\rho_{na}\nu_{na}}} \quad (5)$$

The resulting non-dimensional equations for the analyzed systems are presented below:

-Continuity Equation

$$\frac{\partial U}{\partial X}+\frac{\partial V}{\partial Y}=\ 0 \quad (6)$$

-$X-momentum\ Equation$

$$U\frac{\partial U}{\partial X}+V\frac{\partial V}{\partial Y}=-C_1\frac{\partial P}{\partial X}+C_2\frac{\mu_{nf}}{\rho_{nf}\alpha_f}\left(\frac{\partial^2 U}{\partial X^2}+\frac{\partial^2 U}{\partial Y^2}\right)-C_3\frac{\mu_{nf}}{\rho_{nf}\alpha_f}\frac{U}{Da}+ C_1PrHa^2\left(Vsin(\gamma)cos(\gamma)-Usin^2(\gamma)\right) \quad (7)$$

$$-Y-momentum\ Equation$$

$$U\frac{\partial V}{\partial X}+V\frac{\partial V}{\partial Y}=-C_1\frac{\partial P}{\partial Y}+C_2\frac{\mu_{nf}}{\rho_{nf}\alpha_f}\left(\frac{\partial^2 V}{\partial X^2}+\frac{\partial^2 V}{\partial Y^2}\right)-C_3\frac{\mu_{nf}}{\rho_{nf}\alpha_f}\frac{V}{Da}+C_1\frac{(\rho\beta)_{nf}}{\rho_f\beta_{nf}}Ra\theta+C_1Ha^2Pr\left(Usin(\gamma)cos(\gamma)-Vcos^2(\gamma)\right) \quad (8)$$

$$-Energy\ Equation$$

$$U\frac{\partial \theta}{\partial X}+V\frac{\partial \theta}{\partial Y}=C_4\left(\frac{\partial^2\theta}{\partial X^2}+\frac{\partial^2\theta}{\partial Y^2}\right) \quad (9)$$

The equations for the properties of nanofluid are inserted below:

$$\alpha_{na}=\frac{k_{nf}}{(\rho C_p)_{nf}} \quad (10)$$

$$\rho_{na}=(1-\phi)\rho_f+\phi\rho_p \quad (11)$$

$$(\rho c_p)_{nf}=(1-\phi)(\rho c_p)_f+\phi(\rho c_p)_p \quad (12)$$

$$(\rho\beta)_{na}=(1-\phi)(\rho\beta)_f+\phi(\rho\beta)_{sp} \quad (13)$$

The coefficients shown in equation 7 to equation 9 are as indicated in table 1. The physical and thermal characteristics of water and $Al_2\ O_3$ nanoparticles at 25°C were taken from table 2.

Boundary Conditions

In this work the boundary conditions had been employed in the numerical simulation as below:

- hot circular pipe (Inner), $\theta=1; U=V=0$)
- cold circular pipe (Inner) , $(\theta=0; U=V=0)$
- Insulation (top and bottom) walls;($\frac{\partial\theta}{\partial Y}=0; U=V=0$)

The simulation is applied along the permeable interface between the porous partition and the nanofluid region:

$$\theta_{po}=\theta_{na},\quad \frac{\partial\theta_{na}}{\partial X}=\frac{K_{eff}}{K_{na}}\frac{\partial\theta_{po}}{\partial X},\quad \Psi_{po}=\Psi_{na},\quad \frac{\partial\Psi_{na}}{\partial X}=\frac{\partial\Psi_{po}}{\partial X},\quad \Omega_{po}=\Omega_{na},\quad \frac{\partial\Omega_{na}}{\partial X}=\frac{\partial\Omega_{po}}{\partial X},\quad \mu_{po}\left(\frac{\partial U_{po}}{\partial Y}+\frac{\partial V_{po}}{\partial X}\right)=\mu_{na}\left(\frac{\partial U_{na}}{\partial Y}+\frac{\partial V_{na}}{\partial X}\right),\quad P_{po}=P_{na},\quad \frac{\partial P_{po}}{\partial X}=\frac{\partial P_{na}}{\partial Y} \quad (14)$$

Nusselt numbers is important to mention that, within the present numerical configuration, they are evaluated directly on the inner hot pipe surface. Since this pipe acts as a thermal divider that separates the enclosure into two distinct regions, the Nusselt number is computed individually for the left and right sides, and finally, the overall mean value is obtained.

$$Nu_{loc}=\frac{\partial\theta}{\partial n} \quad (15)$$

$$Nu_{avg}=\frac{1}{2}\left\{\frac{1}{\pi}\left[\frac{k_{na}}{k_{bf}}\right]\int_0^{\pi} Nu_{loc}(\varphi)d\varphi+\frac{1}{\pi}\left[\frac{k_{eff}}{k_{bf}}\right]\int_{\pi}^{2\pi} Nu_{loc}(\varphi)d\varphi\right\} \quad (16)$$

THERMAL BOUNDARY CONDITIONS

An isothermal internal heat source in steady-state is also assumed. This is done by introducing non-dimensional groups based on the characteristic scales which are temperature-related boundary conditions that are taken to be constant and continuous. In particular, we keep the hot source inside this geometry (a circle or star-like body) at a non-dimensional temperature θ□ = 1 and enforce that the cold ones are both fixed to θc = 0. It is noted that this setup corresponds to a uniform heating boundary condition, and it is simplified and numerically stable in natural convection studies.

NUMERICAL MODELING AND VALIDATION

The governing equations solved numerically for under steady-state conditions by applying the finite element (FEM) technique. Setting the convergence criteria to 10^{-5}, the computational mesh was carefully validated for correctness:

$$\frac{\Sigma \left|\xi_{i,j}^{n+1}-\xi_{i,j}^{n}\right|}{\left|\xi_{i,j}^{n+1}\right|} \leq 10^{-5} \qquad (17)$$

The properties in the present study, the thermophysical properties of the $Al_2\ O_3$ –water nanofluid are evaluated based on the mixture model proposed by Tiwari and Das, which is widely used in natural-convection simulations. The properties of nanofluids are determined at three concentration levels of nanoparticles (1%, 2% and 3%) to investigate the effect of particle loading on heat transfer performance. The density, heat capacity, viscosity and thermal conductivity for the nanofluid are calculated using the standard relations of Tiwari and Das which consider solid liquid mixture as a single-phase homogeneous fluid. Increasing the nanoparticles concentration enhances the thermal conductivity of the nanofluid, however, it also increases viscosity which may introduce addition flow resistance. figure 3 illustrated the effect of nanoparticle concentration on the thermal conductivity of the nanofluid, while figure 4 shown the effect of nanoparticle concentrations on viscosity. Also, the thermal conductivity rises almost linearly with concentration suggesting greater heat-transporting ability. Meanwhile, figure 4 shows a general increase in viscosity as expected for nanofluids, and consistent behavior with the data presented by Tiwari and Das. It is important that these variations of thermophysical properties are taken into account when accurate simulations of the thermal performance of heat source in the wavy enclosure are needed, since they directly affect the fluid flow pattern and drainage rate around the internal heat source.

VALIDATION OF NUMERICAL SOLUTIONS

To ensure the reliability of the numerical procedure adopted in the present study, a validation was performed by comparing the obtained results with the benchmark data published by Ali Al-Zamily (2017). In this study the analysis of natural convection and entropy generation in a cavity filled with multi-layers of porous medium and nanofluid with a heat generation was investigated. In the referenced work, natural convection was analyzed for a multilayer enclosure in which the left vertical wall is divided into two equal segments: the lower half subjected to a constant heat flux q", and the upper half thermally insulated. The cavity consists of three regions: a nanofluid layer, a porous central layer of thickness L_pm = L/3, and a second nanofluid layer, while the right wall is maintained at a uniform cold

temperature Tc. For Case-1, Al-Zamily presented streamline patterns and average Nusselt number values at Ra = 107, Da = 10-5, and thermal conductivity ratio λ = 0, for three nanoparticle volume fractions: φ = 0.00, 0.05, 0.10. The corresponding reference values were extracted from the published figure and compared with the results of the present model under the same physical and geometrical conditions. A clear agreement is observed in the streamline behavior (as illustrated in figure 5), where the vortex structure and recirculation intensity exhibit the same qualitative trends reported by Al-Zamily. Similarly, the variation of the average Nusselt number with nanoparticle concentration (shown in figure 6) follows a monotonic increasing trend similar to that of the reference study. A quantitative comparison of the Nusselt number values is summarized in table 5, where the deviations between the two datasets were computed. The maximum percentage error was found to be 5.45%, and the Mean Absolute Percentage Error (MAPE) was 3.24%, both of which fall well within the acceptable limits for numerical validation of natural-convection models at high Rayleigh numbers. These results validate the correctness, stability and accuracy of the current numerical scheme forming a sound base for further numerical studies on more complicated geometries and flow physics to be discussed in Solar transient simulations

$$Error = \frac{Present\ Study - Reference\ Study}{Reference\ Study} \quad (18)$$

RESULTS AND DISCUSSION

The influence numerical experiments were conducted to study the effect of governing dimensionless parameters on the thermal and flow behavior inside the wavy enclosure. The following parametric investigations were conducted:

-Rayleigh test (Ra = 10^4 , 10^5 , 10^6) at fixed Hartmann number (Ha = 60), Darcy number (Da = 10^{-3}) and magnetic field orientation angle (γ = 0°).

-Darcy number test (Da = 10^{-3}, 10^{-4} , 10^{-5}) for constant Ra (=1.0×{10}6), Ha (=60) and magnetic field inclination angle (γ=0°).

-Hartmann number test (Ha = 0, 20, 40, 60) for a fixed Rayleigh number (Ra = 10^6), Darcy number (Da = 10^{-3}), and magnetic field angle (γ = 0°)

-Inclination angle (γ = 0°, 45°, 90°) with constant values of Rayleigh number (Ra = 10^6), Darcy number (Da = 10^{-3}), and Hartmann number (Ha = 60)

- Configuration 1: (a) Centered Circular heat source
- Configuration 2: (b) Vertical heated wall at the center
- Configuration 3: (c) Flower-shaped heat source

These parametric cases were designed to identify which internal heating configuration provides the most effective enhancement of natural convection and flow circulation. The results are interpreted using contour plots of the stream function and complementary graphs and tables, allowing a direct comparison of the three internal geometries under each set of conditions.

Effect of Rayleigh Number on Stream Function in a Porous Medium

The flow regime in a porous enclosure, as depicted in figure 8, exhibits a strong dependence on the Rayleigh number (Ra) that prescribes the strength of natural convection. For Ra <

10^4 the flow is weak and conduction controls heat transfer. They are themselves sparsely populated with the small dim vortices, are of the lowest maximum stream function value across all geometries. At Ra=10^5 convection driven by buoyancy effects, start to become an influence. Both the circular design with a retrace wall heating as well as the wall-heated geometry yield more symmetric and organized recirculating zones, whereas due to its sharp edges, the star-shaped arrangement causes noticeable asymmetry. The flow intensifies as, for all cases, ψmax increases substantially. The influence of natural convection prevails at Ra = 10^6 . Strong and intricate gyroscopic structures emerge, particularly close to the star-shaped configuration where sharp corners tend to concentrate a large local circulation. Stream function has peak contributions at these same conditions showing that a strong convective state is attained even with this obstacle. This is corroborated more quantitatively in figure 9. which displays the convergence of the maximum stream function values as Ra is increased for the three internal geometries. The results highlight the influence of Rayleigh number (Ra) on transition from conduction to convection heat transfer. Second, it highlights that the form of heat source and porosity resistance acting together govern features such as strength, symmetry and complexity in flow patterns.

Effect of Hartmann Number

Figure 10 represents the impact of Hartmann number on flow pattern in the porous enclosure with three internal geometric configurations (Case–1: circular heat source, Case–2: vertical heated wall, and Case–3: star-like heat sources). At Ha = 0 natural convection develops unrestricted by any magnetic resistance, and the vortical cells are strong and coherently defined. As the large wall is heated, buoyancy-driven motion increases. The strongest circulation develops in Case 2 when ψ_max ≈ 35.698. Case 3 also presents a stronger recirculating flow generated by its sharp corners; the Case 1 detachment is smoother and weaker. As Ha is further increased to 40 and 60, the flow in all cases is strongly inhibited. The Lorentz force damps fluid motion, reducing the size and strength of vortices to an appreciable extent. Maximum damping is found for Case 1 (circular source) and suggests that smooth geometries are more affected by magnetic suppression. In contrast, Case 3 (starlike source) keeps relatively high circulation at large Ha values. For the jagged edges, local acceleration zones are formed (which give rise to sustainable rotation despite magnetic damping). The total circulation strength at high Ha reads:

- Case 3 > Case 2 > Case : This means that the geometrical complexity promotes natural convection as well as weakens stabilizing effect of magnetic field. These trends show that the magnetic field successively restricts the rotation in porous medium, which can further be perceived from figure 11 where ψ_max decreases continuously by increasing Ha; it is also noticeable that star-shaped geometries as a matter of fact again demonstrate a maximum circulation respectively for all cases analyzed.

Effect of Darcy's Number

The impact of the Darcy number on the intensity of the flow in the porous region is well-reflected from figure 12, the numerical tendency of ψ_max is supported in figure 13. Three different porosities were considered: Da = 10^{-3}, 10^{-4} and 10^{-5} at identical operating parameters (Ra = 10^6 , H a = 60, γ =45°). At the largest values of Da = 10^{-3}, the porous layer at most facilitates the movement of the fluid. Well-defined and active vortices are

observed, particularly at the star-shaped heat source region where we find ψ_max = 13.767 which signifies a regime of strong buoyancy-driven convection. When the permeability is further decreased to Da = 10^{-4} , a porous medium starts to retard movement ofthe fluid. Streamlines are depopulated and the circulation weakens significantly. The peak values decrease to: Case 2: ψ_max = 3.2626. Case 3: ψ_max = 2.5448 indicating the weaker convective activity with weakening flow resistance. At the slowest permeability (Da = 10^{-5}), the porous medium is nearly equivalent to a solid obstacle. A weak flow is apparent, and the system approaches a conduction-dominated.

Effect of inclination angle

The effect of magnetic field angle inclination on the strength of flow can be vividly seen from the streamline plot (figure 14) and later confirmed by varying ψ_max presented in figure 15. Three different inclination angles; γ = 0°, 45° and 90° were investigated at fixed Ra = 10^6 , Ha=60 and Da=10^{-3}. For γ = 0°, the magnetic field is oriented horizontally and circulation patterns are nearly symmetric. The strongest vortex (ψ_max = 11.519) develops in the VWF, and weaker motion is observed for CWS (ψ_max = 4.4855) and SSWF (ψ_max = 5.0883). This suggests Lorentz forces have a negligible disruption effect on the buoyancy-driven flow at this configuration. At γ = 45°, there is a Lorentz contribution induced by the magnetic field which favors diagonal recirculation. In all cases, the flow becomes stronger and the strength reaches its maximum value (ψ_max = 13.767) for the star-shape source. This angle provides the most efficient convection, since the inclined magnetic field will help to build up vortical motions rather than inhibiting those. At γ = 90°, the magnetic field is vertical and it pushes directly against the vertical buoyancy forces. This alignment profoundly modifies the flow structure, particularly given that in the wall-heated case a maximum circulation was achieved (ψ_max = 16.824). For the circular and star sources average vortex activity is moderately small (ψ_max = 8.0305 and 11.218), but overall circulation increases, because Lorentz forces are preferentially oriented in the vertical direction. The trend summarized in figure 15, the maximum value of ψ increases monotonously with the change of γ from 0° to 45° for all three cases, peaks depending on geometry and then redistributes at 90° due to magnetic and buoyancy forces being totally aligned. This demonstrates that the inclination angle not only changes convection paths, but can amplify or reduce circulation depending on its alignment with gravity.

CONCLUSION

In this paper we calculated some qualitative and quantitative behaviors of IHSG, internal heat source dimensionality and key physical parameters figure 7 (i.e., the Rayleigh number (Ra), Hartmann number (Ha), Darcy number (Da) and magnetic-field inclination angle(γ)) on natural convection in a wavy corrugated enclosure filled with nanofluid and containing a central porous region. The findings reveal the intertwined influence of geometric complexity, buoyancy forces, magnetic damping, and porous-medium resistance on the heat–flow performance. The circulation of star-shaped heat source is the maximum one among these three cases and can reach ψ_max ≈ 13.76 with Ra = 10^6 and γ = 45°, which indicates that this geometry has enhanced promoting effect for the development of strong buoyancy-induced flow than others on account of its sharp corners and increased thermal boundary. Conversely, the circular shape heat source leads to the lowest flow structures

($\psi_{max} \approx 9.99$) and the vertical heated wall performs as an intermediate situation ($\psi_{max} \approx 10.33$). These results verify that the convective intensity and heat transferring capacity can be increased when geometrical complexity of porous material increases. The role of Hartmann number was clearly a damping action; at Ha = 0, the natural convection was manifested in the strong vortical phenomena depicted with higher circulation ($\psi_{max} \approx 35.7$ for star shape). Flow magnitude continued to decrease as Ha was further increased to 40 and 60, because of Lorentz-force stabilization, with the value for $\psi_{max} \approx 16.28$ and ~10.33 obtained correspondingly. This shows the potential for magnetic field to quench convective motion and move the system towards a conduction-controlled regime. The flow of permeability was governed by the Darcy number. For $Da = 10^{-3}$, strong convection was observed with well-developed recirculating cells, and at lower permeabilities ($Da = 10^{-4}$ and 10^{-5}) there is three orders of magnitude reduction in the circulation (ψ_{max} declined from $13.767 \rightarrow 3.2626 \rightarrow 0.82238$), suggesting the transition from regime one conduction enhancement to two conduction dominated behavior.

Finally, the inclination angle γ demonstrated that magnetic-field orientation could support or inhibit flow strength depending on the direction of Lorentz and buoyancy forces. The greatest increment was at $\gamma = 45°$ for complex shapes, i.e. star shape, $\gamma = 90°$ produced maximum circulation ($\psi_{max} \approx 16.82$) for vertically heated wall. Thus, the presentation25 shows that best thermal performance lies in simultaneous optimization of geometry as well as magnetic-field alignment. In general, we find that geometry, permeability, magnetic field strength and orientation have a joint effect in controlling the flow pattern as well as the heat transfer process. The star-shaped heat device is demonstrated to be the most effective in enhancing the convection, especially at large Rayleigh numbers and oblique magnetic angles that may impose a hopeful alternative for practical thermal management applications.

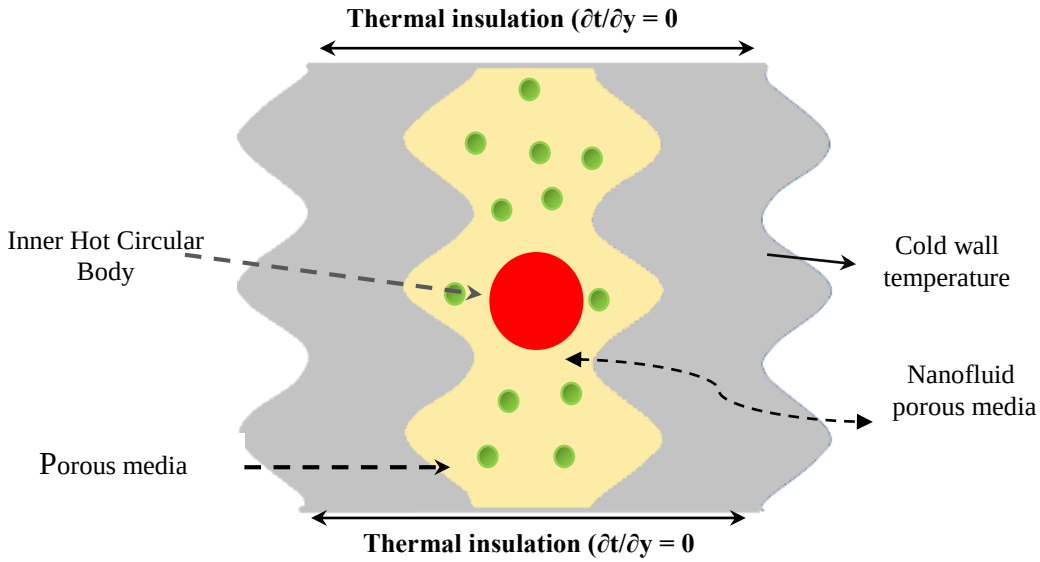

Fig. 1. Schematic 2D numerical model with porous and nanofluid regions.

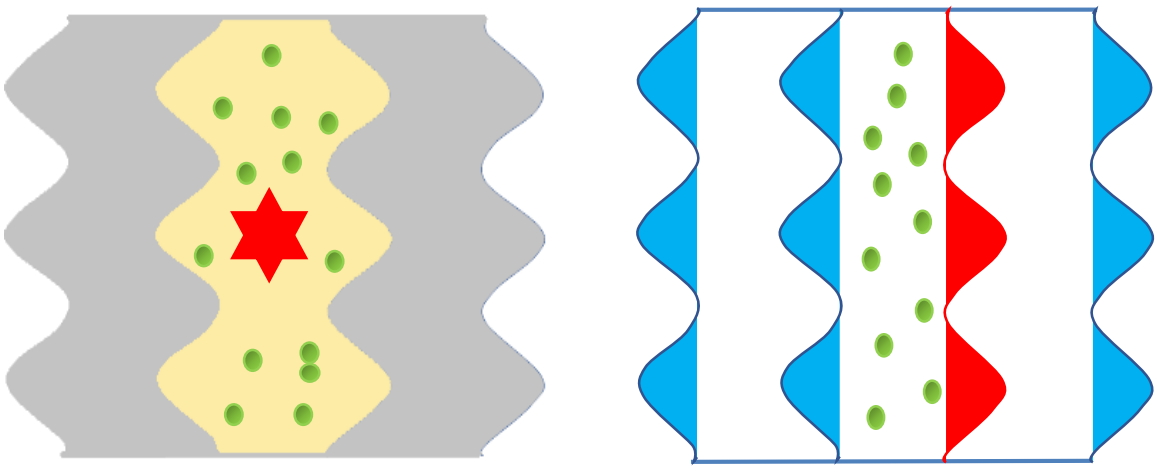

(a) **(b)**

Fig. 2. Two heat sources—(a) star-shaped internal heater embedded in a porous zone, (b) vertical heated wall applied to the side of a wavy enclosure of the 2D numerical model.

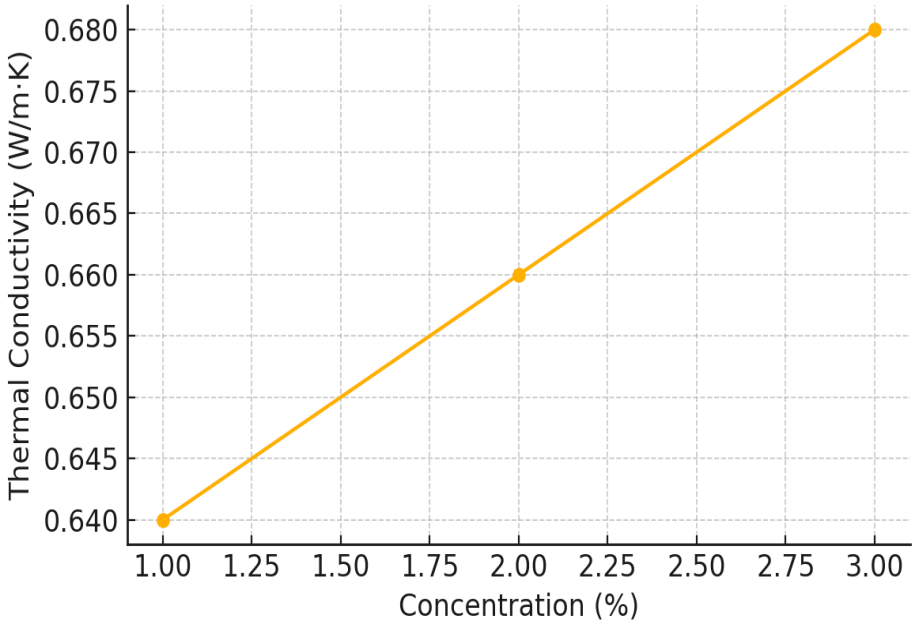

Fig. 3. Effect the nanoparticle concentration on the thermal conductivity.

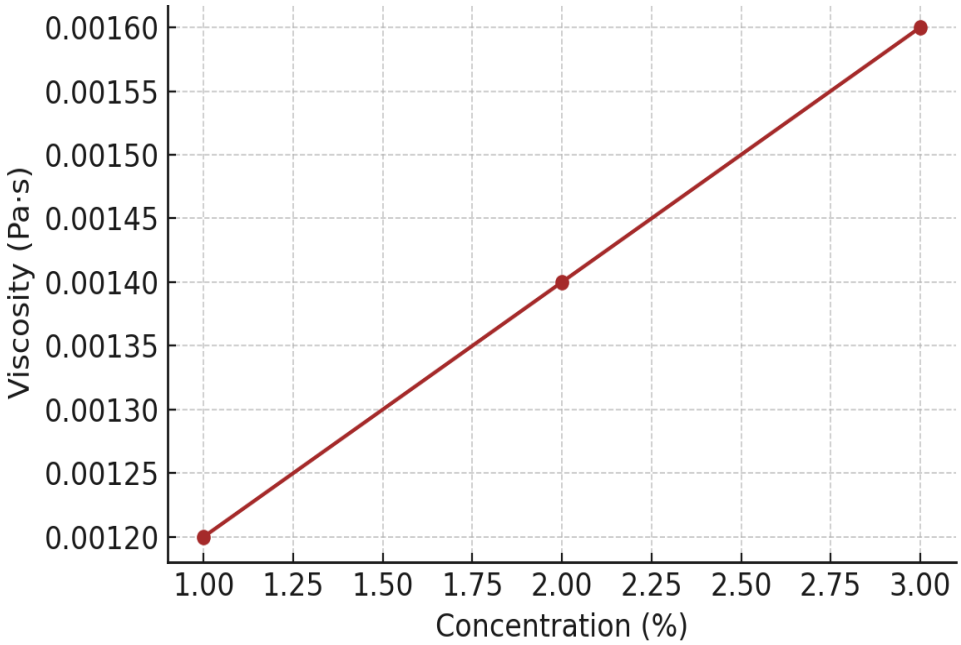

Fig. 4. Effect of the nanoparticle concentration on the viscosity.

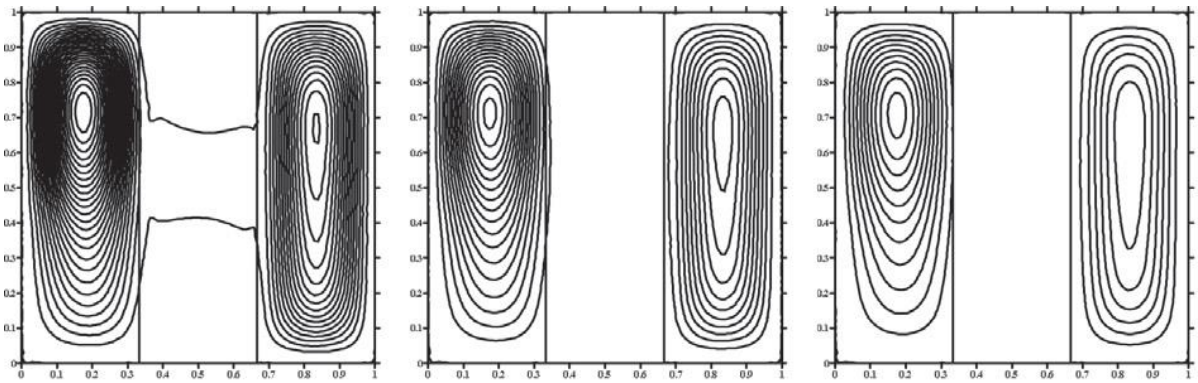

(b) Ali Al-Zamily

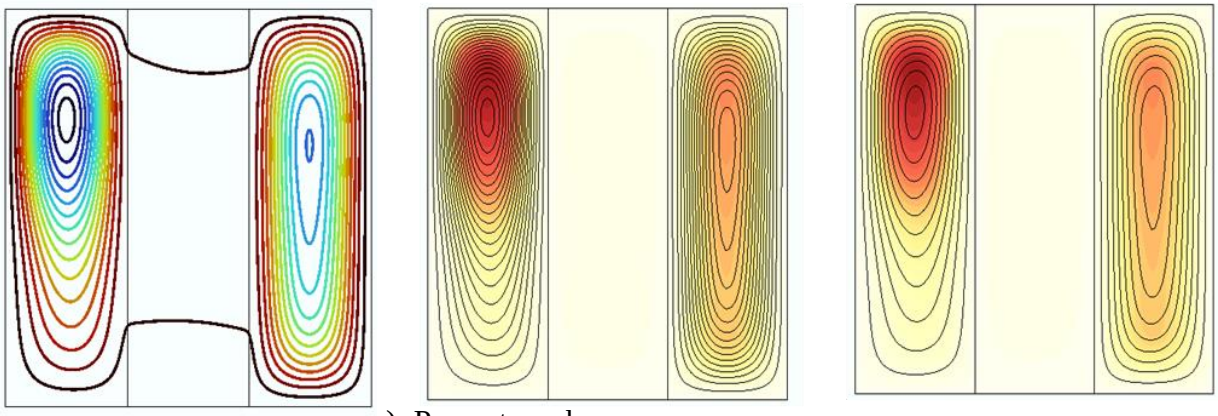

(c) Present work

Fig. 5. Validation of streamlines using numerical results: (a) Ali Al-Zamili; (b) Corresponding result from the present study at the same parameters.

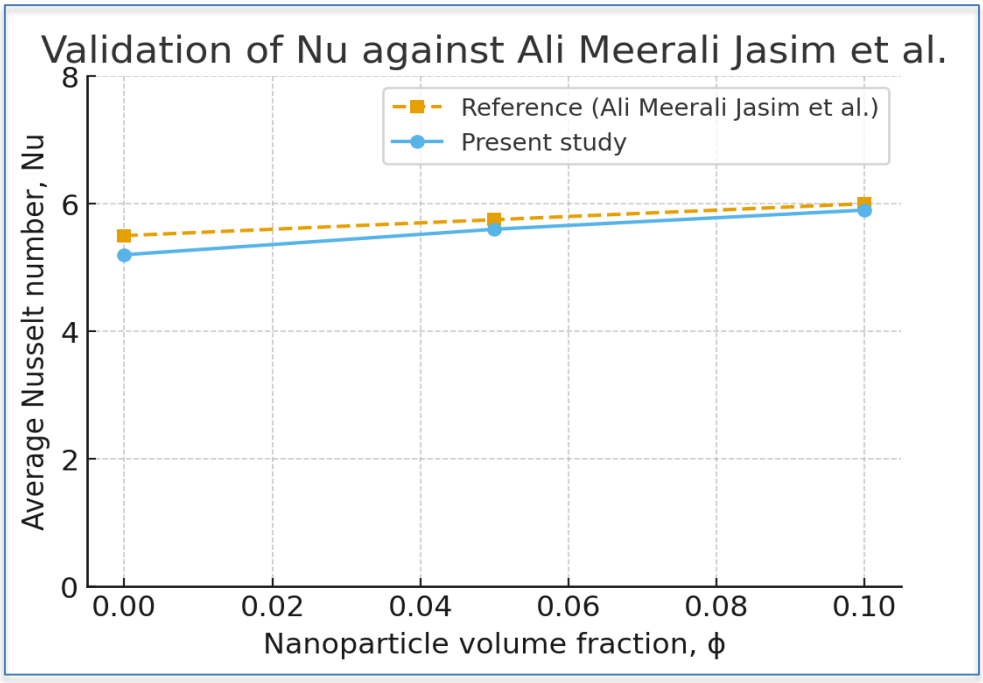

Fig. 6. Comparison of Nusselt number between present Study and Ali Al-Zamily at Ra = 10^7.

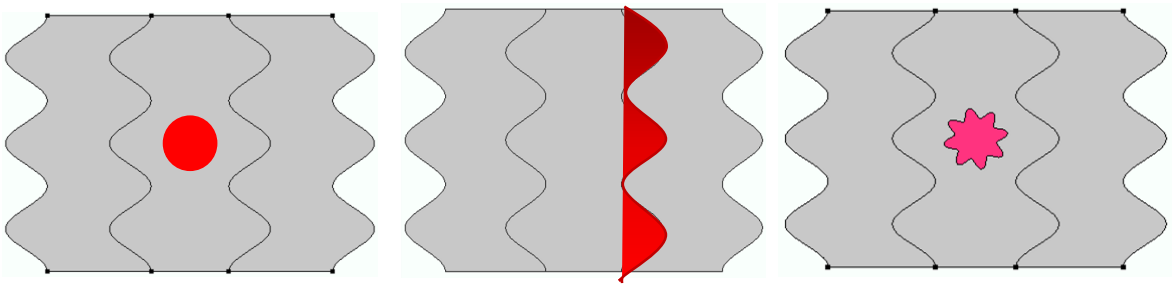

(a) **(b)** **(c)**

Fig. 7. (a) Circular heat source. (b) Vertical heated wall at center (middle). (c) Flower-shaped heat source. Assessment of internal heat source geometries on stream function behavior at high thermal conditions (Ra = 10^6 , Ha = 60, Da = 10^{-3}, γ = 45°, φ = 0.04).

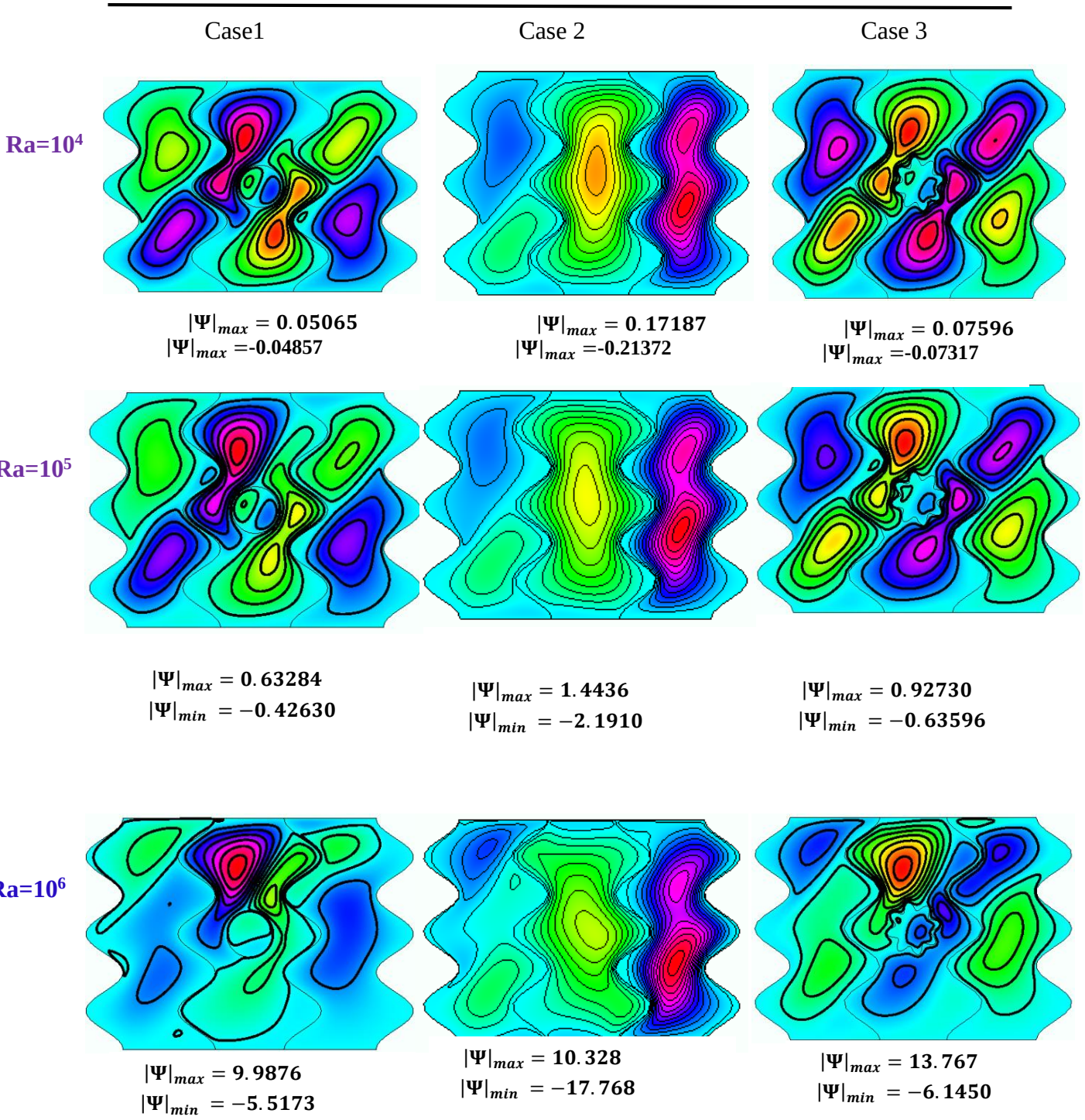

Fig. 8. Stream functions for different Rayleigh number (at Ha= 60, ε= 0.4 γ = 45^{o}, and Da= 10^{-3}).

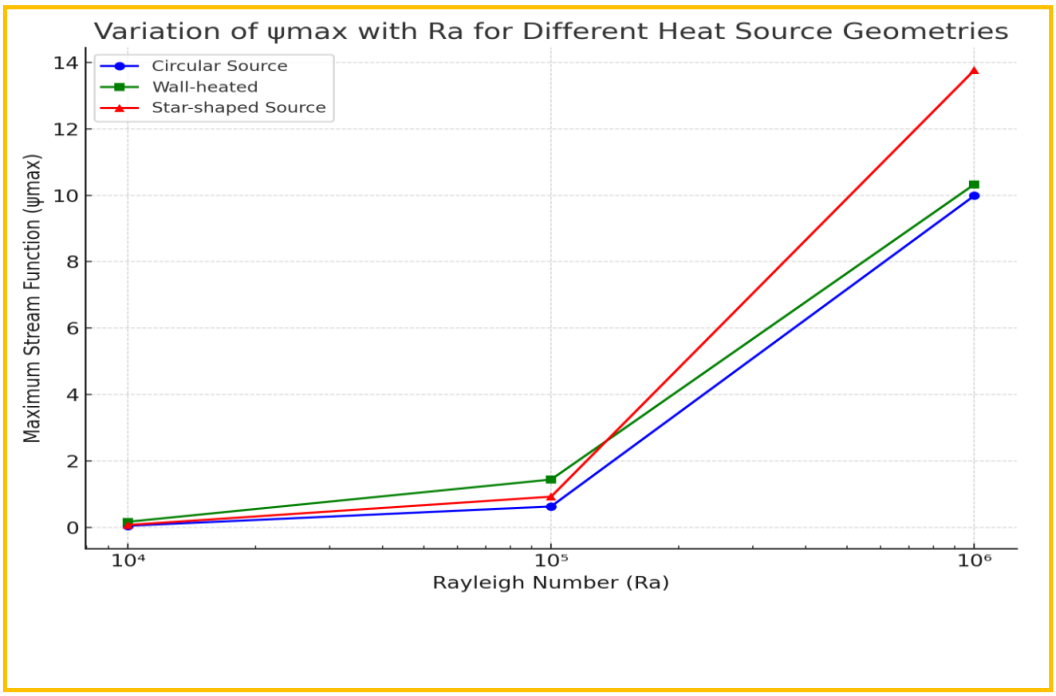

Fig. 9. Maximum stream function (ψ_{max}) variation with Ra number for different heat source geometries, with annotated values to highlight differences.

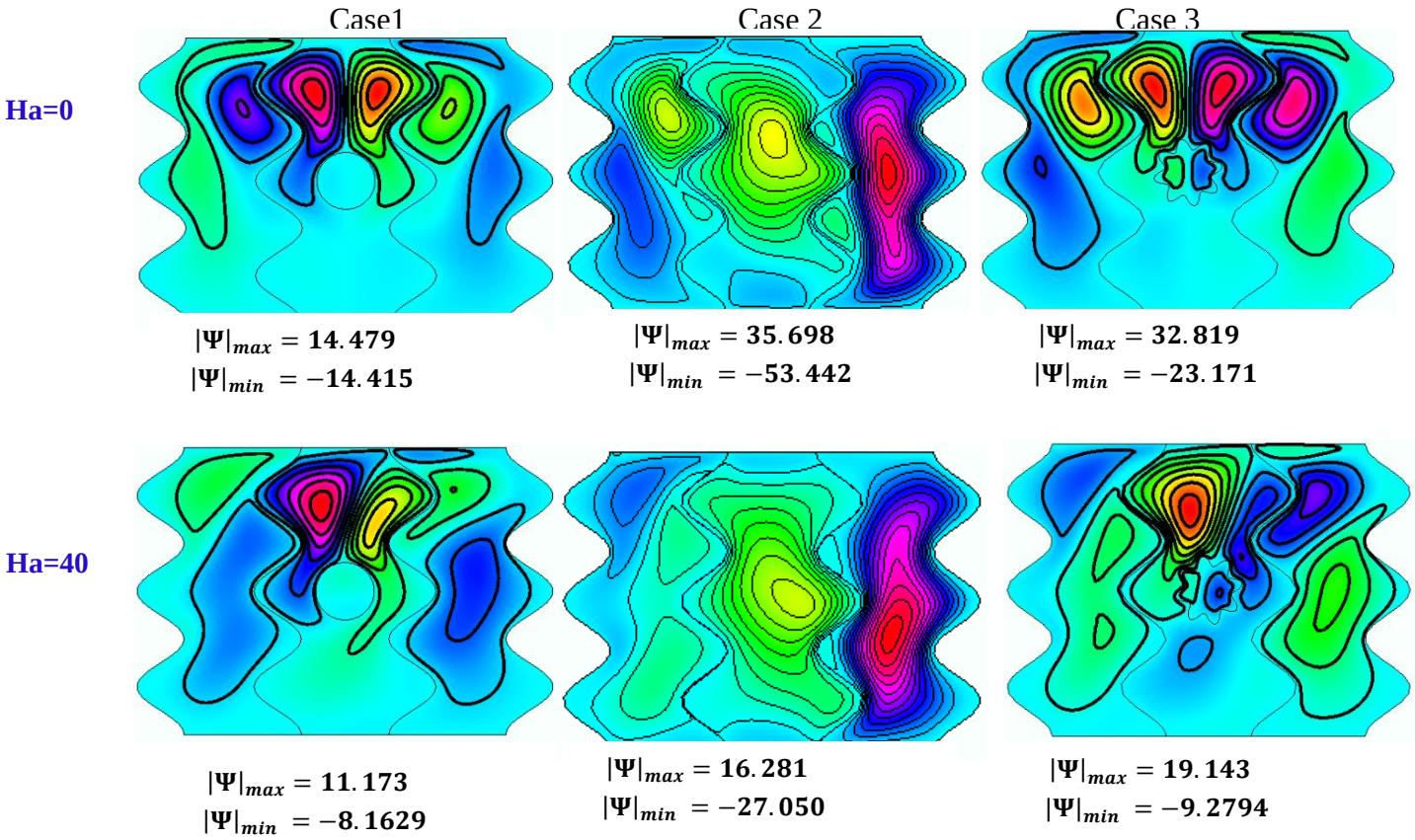

Ha=60

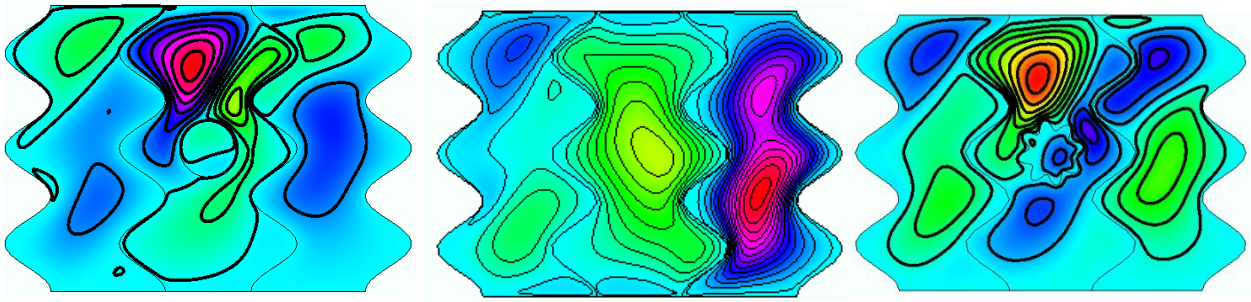

$|\Psi|_{max} = 9.9876$
$|\Psi|_{min} = -5.5173$

$|\Psi|_{max} = 10.328$
$|\Psi|_{min} = -17.768$

$|\Psi|_{max} = 13.767$
$|\Psi|_{min} = -6.1450$

Fig. 10. Stream function counter for different Hartmann (Ha) numbers (at Ra= 10^6, ε= 0.4, γ = 45°, and Da= 10^{-3}).

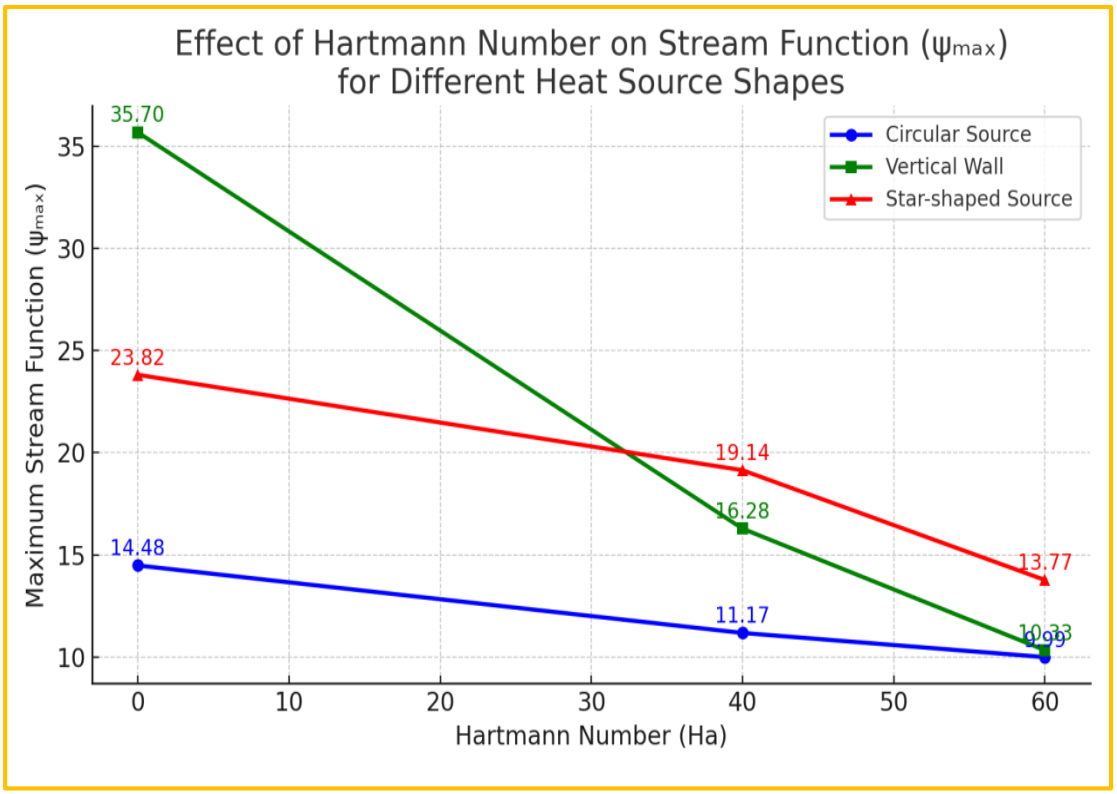

Fig. 11. Maximum stream function (ψ□ax) variation with Hartmann number for different heat source geometries, with annotated values to highlight differences.

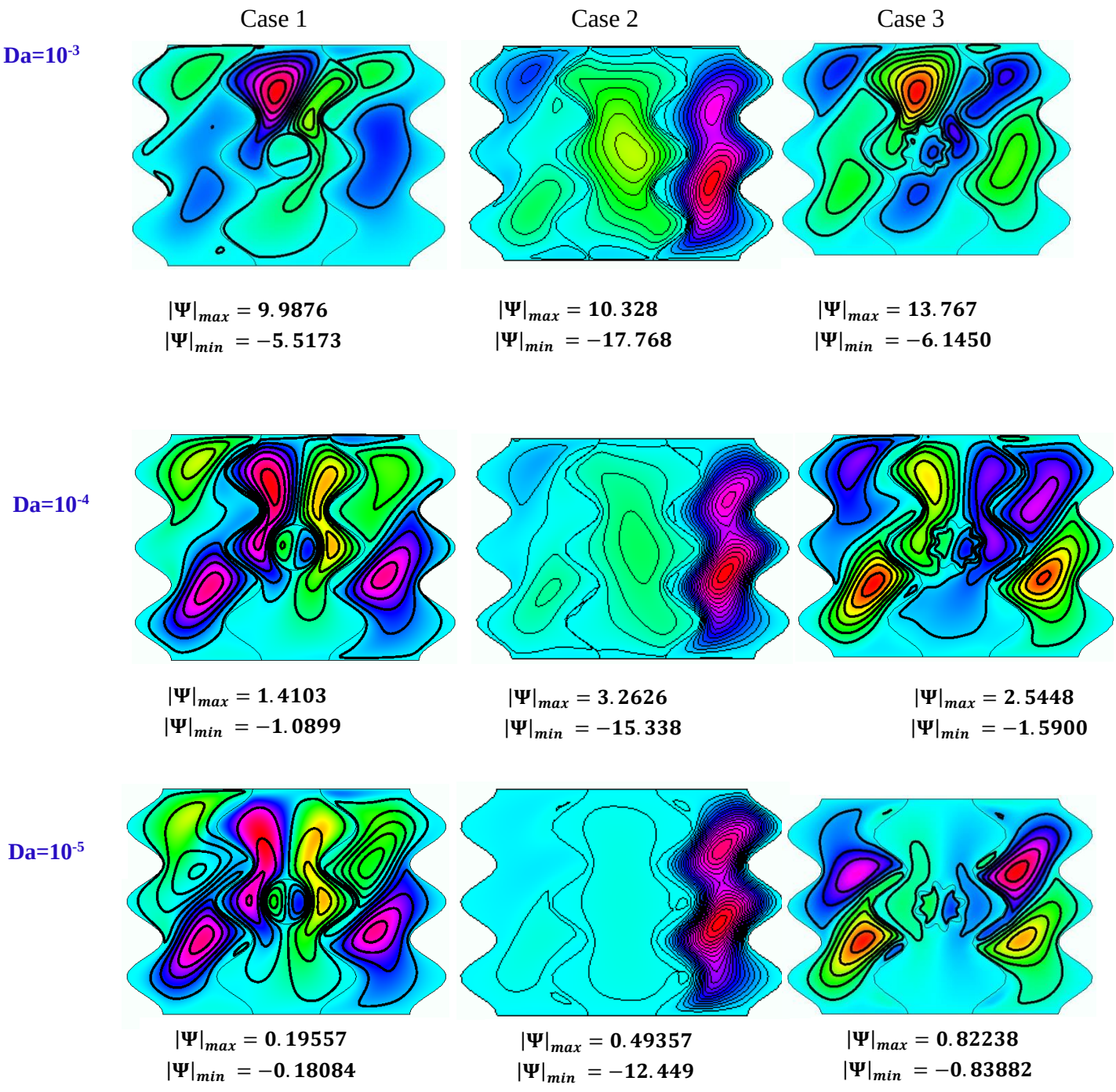

Fig. 12. Stream function counter for different Darcy (Da) numbers (at Ra= 10^6 and γ = 45° Ha= 60).

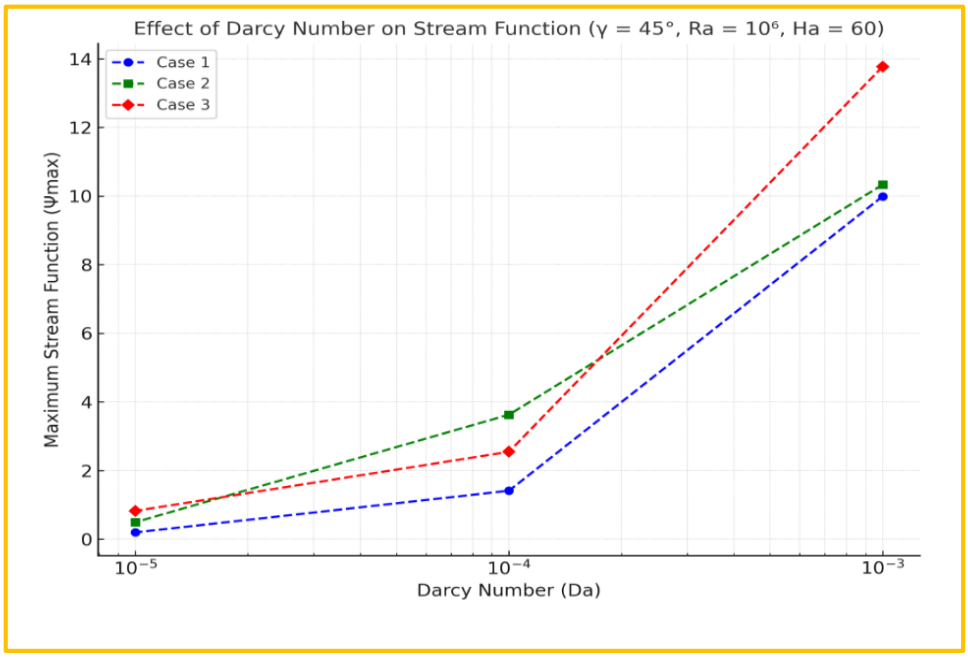

Fig. 13. Variation of ψmax with Darcy number for different cases.

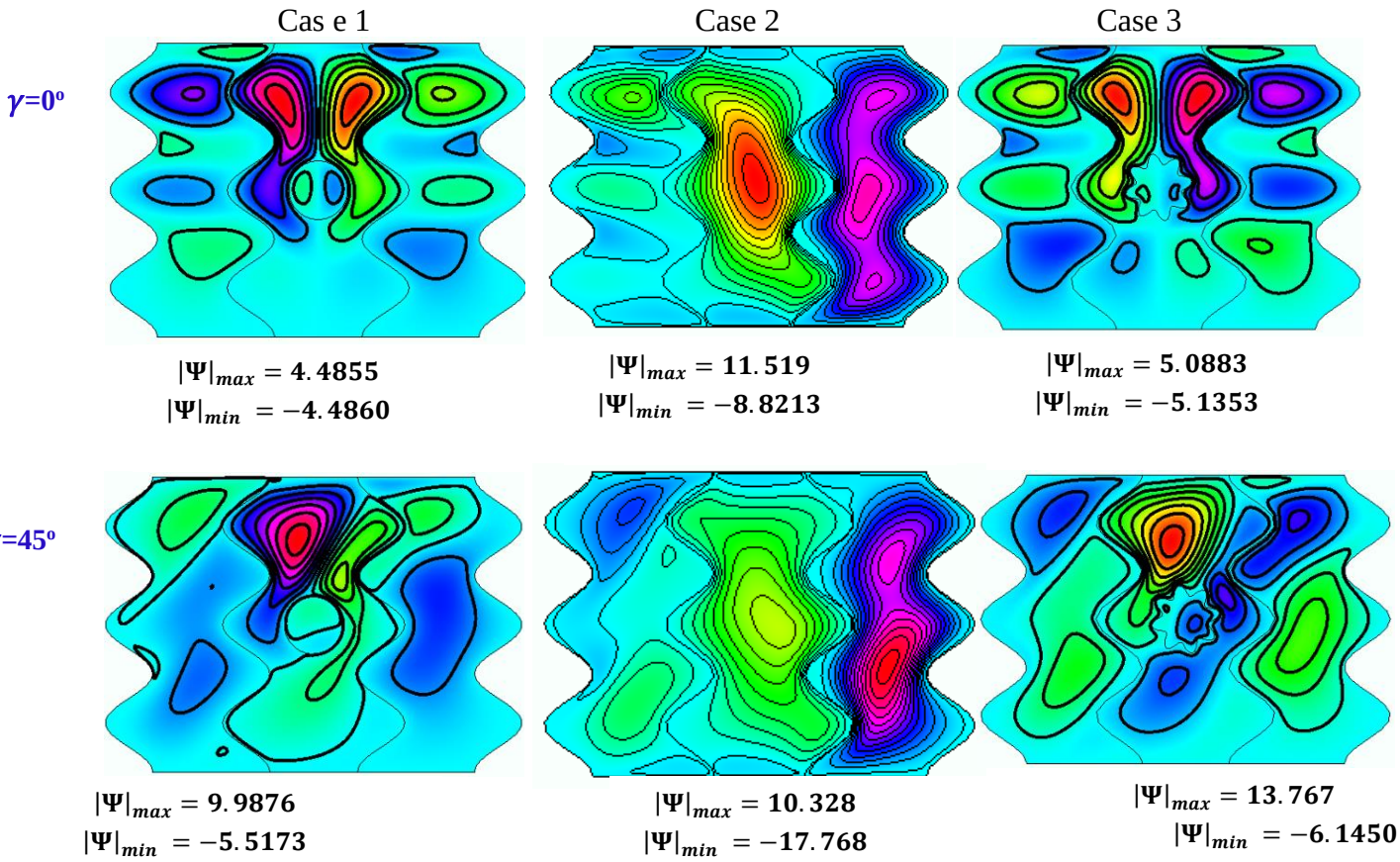

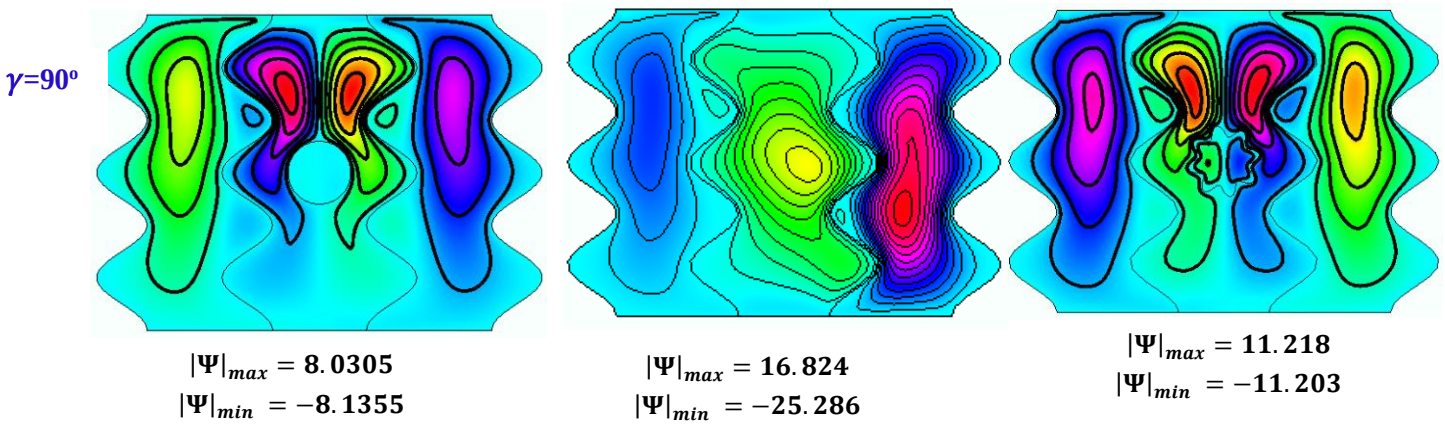

Fig. 14. The stream function counter varies the magnetic source's inclination angle (Ha=60, Ra=10^6, Da=10^{-3}).

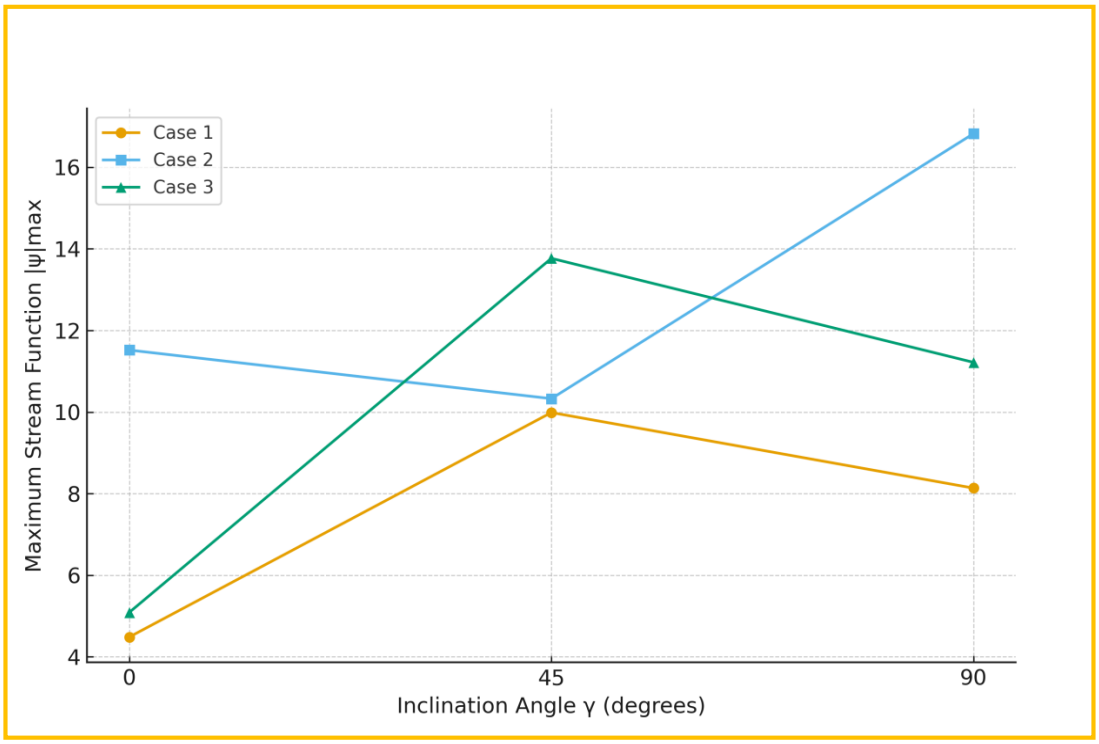

Fig. 15. Variation of |ψ|max with inclination angle (γ).

Table 1. Properties of coefficient constant of nanofluid and nano-porous layers.

Layer	C_1	C_2	C_3	C_4
Nanofluid Layer	1	1	0	$\frac{\alpha_{nf}}{\alpha_f}$
Nano-Porous Layer	ε^2	ε	ε^2	$\frac{\alpha_{eff}}{\alpha_f}$

Table 2. Thermo-physical properties of water and nanoparticles (Al_2O_3) at T=25°C

.

Properties	ρ (kg/m³)	Cp (J/kg.K)	k (W/m.K)	β (1/K)
Water	997	4180	0.614	$2.1*10^{-4}$
Al_2O_3	3970	765	40**0**	$0.85*10^{-5}$

Table 3. Parameters and values for thermal boundary conditions.

Parameter	Description	Value
θ	Non-dimensional hot surface temperature	1
θ	Non-dimensional cold wall temperature	0
Heat Source Type	Thermal condition in hot region	Continuous, Isothermal

Table 4. Thermophysical properties of Al_2O_3 /Water nanofluids at different concentrations.

Concentration (%)	Thermal Conductivity (W/m·K)	Viscosity (Pa·s)
1.0	0.64	0.0012
2.0	0.66	0.0014
3.0	0.68	0.0016

Table 5. Comparison between the present study and Ali Al-Zamily at Ra = 10^7.

Nanoparticle Volume Fraction (ϕ)	Reference Study	Precent study	Percentage change %
0.00	5.5	5.20	5.45%
0.05	5.75	5.60	2.61%
0.10	6	5.90	1.67%

REFERENCES

Abdulkadhim, A., Abed, I.M., and Said, N.M., "Computational investigation of magnetohydrodynamics convective heat transfer in I-shaped wavy enclosure considering various shapes of inner bodies filled with nanofluid–porous layers", Brazilian Journal of Chemical Engineering, vol. 40, No. 2, PP. 427–447, June 2023. doi.org/10.1007/s43153-022-00251-5

Abdulkadhim, A., Abed, I.M., and Said, N.M., "Experimental investigation of heat transfer for nanofluid–porous magnetohydrodynamic thermally driven flow in a novel I-shaped enclosure", Journal of Thermal Analysis and Calorimetry, vol. 148, No. 13, PP. 6207–6221, 2023. doi.org/10.1007/s10973-023-12069-5

A. M. Rashad, Ali J. Chamkha, Muneer A. Ismael, Taha Salah , "Magnetohydrodynamics Natural Convection in a Triangular Cavity Filled With a Cu-Al2O3/Water Hybrid Nanofluid With Localized Heating From Below and Internal Heat Generation", Journal of Heat Transfer, vol. 140, No. 7, pp. 209–219, 2018. doi.org/10.1115/1.4039213

Ammar Abdulkadhim Fathi Saeed, "Magneto-hydrodynamic Natural Convection in I-Shaped Wavy Walls Enclosure Partially Inserted with Nano Fluid-Porous Media", Ph.D. Thesis, University of Babylon, Iraq, 2022.

Ali Meerali Jasim Al-Zamily, "Analysis of natural convection and entropy generation in a cavity filled with multi-layers of porous medium and nanofluid with a heat generation", International Journal of Heat and Mass Transfer, vol. 106, 2017, pp. 1218–1231. https://doi.org/10.1016/j.ijheatmasstransfer.2016.10.102

Ali Malekpour, Nader Karimi, and Amirfarhang Mehdizadeh, "Magnetohydrodynamics, natural convection, and entropy generation of CuO–water nanofluid in an I-shape enclosure—a numerical study", Journal of Thermal Science and Engineering Applications, vol. 10, no. 6, p. 061016, 2018. doi.org/10.1115/1.4041267

B. Ghasemi and S. M. Aminossadati, "Natural Convection Heat Transfer in an Inclined Enclosure Filled with a Water-Cuo Nanofluid", Numerical Heat Transfer, Part A: Applications, vol. 55, No. 8, pp. 807-823, 2009. https://doi.org/10.1080/10407780902864623

Ching-Chang Cho, Chieh-Li Chen, and Cha'o-Kuang Chen, "Natural convection heat transfer and entropy generation in wavy-wall enclosure containing water-based nanofluid", International Journal of Heat and Mass Transfer, vol. 61, June 2013, Pages 749-758, 2013. doi.org/10.1016/j.ijheatmasstransfer.2013.02.044

E. Abu-Nada and A.J. Chamkha, "Effect of nanofluid variable properties on natural convection in enclosures filled with a CuO-EG-water nanofluid", International Journal of Thermal Sciences, vol. 49, No. 12, pp. 2339–2352, 2010. doi.org/10.1016/j.ijthermalsci.2010.07.006

Farid Berrahil, Abdelkader Filali, Fateh Mebarek-Oudina, Smail Benissaad, Sami Ullah Khan, Cherifa Abid, Salah Saouli, & Yassine Demagh, "Analysis of enhanced

magnetohydrodynamic natural convection in a non-Darcy porous cavity with alumina-water fluid and conductive baffles", International Journal of Numerical Methods for Heat & Fluid Flow, vol. 35, No. 7, PP. 2608–2645, 2025. doi.org/10.1108/HFF-01-2025-0026

Grobler C., Sharifpur M., Ghodsinezhad H., Capitani R., and Meyer J.P., "Experimental study on cavity flow natural convection in porous medium, saturated with an Al_2 O_3 60% EG-40% water nanofluid," Conference: 11th International Conference on Heat Transfer, Fluid Mechanics and Thermodynamics, July 2015.

H.F. Oztop and E. Abu-Nada, "Numerical study of natural convection in partially heated rectangular enclosures filled with nanofluids", International Journal of Heat and Fluid Flow, vol. 29, No. 5, pp. 1326–1336, 2008. doi.org/10.1016/j.ijheatfluidflow.2008.04.009

Isam Mejbel Abed, Farooq H. Ali, and Shaymaa Abdul Munem Sahib, "Investigation of heat transfer and fluid flow around sinusoidal corrugated circular cylinder for two-dimensional system", Frontiers in Heat and Mass, vol. 15, No. 6, PP. 1-9, 2020. doi.org/10.5098/hmt.15.6

J. Mackolil and B. Mahanthesh, "Optimization of heat transfer in the thermal Marangoni convective flow of a hybrid nanomaterial with sensitivity analysis", Applied Mathematics and Mechanics, vol. 42, pp. 1663–1674, 2021. doi.org/10.1007/s10483-021-2784-6

Khalil Khanafer and Kambiz Vafai, "A critical synthesis of thermophysical characteristics of nanofluids," *International Journal of Heat and Mass Transfer", vol. 54, No. 19-20, pp. 4410–4428, 2011. doi.org/10.1016/j.ijheatmasstransfer.2011.04.048

Khan, N. Z., & Bilal, S., "Analyzing dynamics of hybrid nanofluid in curved corrugated enclosure configuring the impact of heated inner cylinder through multigrid simulations", Multiscale and Multidisciplinary Modeling, Experiments and Design, vol.8, No.1, 2024. doi.org/10.1007/s41939-024-00603-3

Lotfi Snoussi Noureddine Ouerfelli, Xavier Chesneau, Ali J. Chamkha, Fethi Bin Muhammad, Amenallah Guizani, "Natural Convection Heat Transfer in a Nanofluid Filled U-Shaped Enclosures: Numerical Investigations", Heat Transfer Engineering, vol.39, Issue 16, pp. 1450-1460, 2018. doi.org/10.1080/01457632.2017.1379343

L.Y. Zhang, R.J. Duan, Y. Che, Z. Lu, X. Cui, L.C. Wei, L.W. Jin, "A numerical analysis of fluid flow and heat transfer in wavy and curved wavy channels", International Journal of Thermal Sciences, vol. 171, 107248, 2022. doi.org/10.1016/j.ijthermalsci.2021.107248

M. Sheikholeslami, A. Arabkoohsar, K.A.R. Ismail, "Entropy analysis for a nanofluid within a porous media with magnetic force impact using non-Darcy model", International Communications in Heat and Mass Transfer, vol. 112, 104488, 2020. doi.org/10.1016/j.icheatmasstransfer.2020.104488

M. Hatami, "Numerical study of nanofluids natural convection in a rectangular cavity including heated fins", Journal of Molecular Liquids, vol. 233, PP. 1-8, 2017. doi.org/10.1016/j.molliq.2017.02.112

M. Muthtamilselvan, P. Kandaswamy, and J. Lee, "Heat transfer enhancement of copper-water nanofluids in a lid-driven enclosure", International Communications in Heat and Mass Transfer, vol. 15, No. 6, pp. 1501–1510, 2010. doi.org/10.1016/j.cnsns.2009.06.015

Mostafa Mahmoodi, "Numerical simulation of free convection of nanofluid in a square cavity with an inside heater", International Journal of Thermal Sciences vol. 50, No. 11, PP. 2161-2175, 2011. doi.org/10.1016/j.ijthermalsci.2011.05.008

Mohsen Sheikholeslami and Davood Domiri Ganji, "Unsteady nanofluid flow and heat transfer in presence of magnetic field considering thermal radiation", vol. 37, PP. 895–902, 2015. doi.org/10.1007/s40430-014-0228-x

M. Chandrasekar, S. Suresh, and A. Chandra Bose, Experimental investigations and theoretical determination of thermal conductivity and viscosity of Al_2 O_3 /water nanofluid", Experimental Thermal and Fluid Science, vol. 34, No. 2, pp. 210–216, 2010. doi.org/10.1016/j.expthermflusci.2009.10.022

Nehad Abid Allah H, Fawzi Sh. Alnasur, Ammar Abdulkadhim, Isam Mejbel Abed, Nejla Mahjoub Said, and Azher M. Abed, "MHD natural convection in a wavy nanofluid enclosure with an internally corrugated porous cylinder," Journal of Taibah University for Science, vol. 18, No. 1, 2024 . doi/10.1108/hff-07-2024-0494

Qusay Rasheed Al-Amir, Ammar Abdulkadhim, Saba Y. Ahmed, Farooq H. Ali, Azher M. Abed, Isam Mejbel Abed, Farooq H. Ali, and Shaymaa Abdul Munem Sahib, "Numerical study of fluid structure interaction of four flexible fins inside nanofluid-filled square enclosure containing hot circular cylinder," Journal of Thermal Analysis and Calorimetry, vol. 147, No. 23, PP. 13999–14017, 2022. doi.org/10.1007/s10973-022-11535-w

Raj Kamal Tiwari, Manab Kumar Das, "Heat transfer augmentation in a two-sided lid-driven differentially heated square cavity utilizing nanofluids", International Journal of Heat and Mass Transfer, vol.50, PP. 2002–2018, 2007. https://doi.org/10.1016/j.ijheatmasstransfer.2006.09.034

Sheremet, M.A., Oztop, H.F., Pop, I., and Al-Salem, K., "MHD free convection in a wavy open porous tall cavity filled with nanofluids under an effect of corner heater," International Journal of Heat and Mass Transfer, vol. 103, pp. 955–964, 2016. doi.org/10.1016/j.ijheatmasstransfer.2016.08.006

Shantanu Dutta, Sukumar Pati, László Baranyi, "Numerical analysis of magnetohydrodynamic natural convection in a nanofluid-filled quadrantal enclosure," Case Studies in Thermal Engineering vol.28, 101507, 2021. doi.org/10.1016/j.csite.2021.101507

Sohail Nadeem, M. Arif, Inayat Ullah and Jehad Alzabut, "MHD natural convection of nanofluid flow using a corrugated permeable medium within corrugated circular cavity," Journal of Thermal Analysis and Calorimetry, vol. 150, PP. 5697–5724, 2025. doi.org/10.1007/s10973-025-14032-y

Yimin Xuan, Qiang Li, "Heat transfer enhancement of nanofluids," International Journal of Heat and Fluid Flow, vol.21, No. 1, pp. 58–64, 2000. doi.org/10.1016/S0142-727X(99)00067-3

Zahra Abdelmalek, Khalil Ur Rehman, Qasem M. Al-Mdallal, Wael Al-Kouz, M.Y. Malik, "Thermal influence of homogeneously heated Y-shaped flipper on flowing stream in an unwavering rectangular domain," Case Studies in Thermal Engineering vol.21, 100715. 2020. doi.org/10.1016/j.csite.2020.100715